A novel interface circuit for grounded capacitive sensors with feedforward-based active shielding

Ferran Reverter[1,2], Xiujun Li[2] and Gerard C M Meijer[2]

[1] Castelldefels School of Technology (EPSC), Technical University of Catalonia (UPC), Avda Canal Olímpic s/n, 08860 Castelldefels, Barcelona, Spain
[2] Electronic Instrumentation Laboratory, Delft University of Technology (TU Delft), Mekelweg 4, 2628 CD Delft, The Netherlands

E-mail: reverter@eel.upc.edu

Abstract
This paper proposes and analyses a novel interface circuit for capacitive sensors in which one of the electrodes is grounded. The novel design makes a charge-balanced relaxation oscillator (applied so far to floating capacitive sensors) suited for the measurement of grounded capacitive sensors and applies advanced measurement techniques, such as auto-calibration and chopping. Furthermore, these techniques are combined with feedforward-based active shielding instead of the usual feedback-based one, thus avoiding instability problems. A prototype of the novel interface circuit has been implemented with discrete components and tested for sensor capacitances between 27 pF and 330 pF and for different lengths of the interconnecting cable. The nonlinearity error amounts to less than 0.1% FSS for a 10 m cable.

Keywords: sensor electronic interface, capacitive sensor, relaxation oscillator, active shielding

(Some figures in this article are in colour only in the electronic version)

1. Introduction

Capacitive sensors are increasingly common in laboratory and industrial measurements to sense pressure, acceleration, humidity, level, distance, among others [1, 2]. Such sensors can be classified into two groups [3, 4]: floating capacitive sensors (i.e. sensors in which neither of the electrodes is grounded) and grounded capacitive sensors (i.e. sensors in which one of the two electrodes is grounded). The former are preferable since they can be read by interface circuits that are intrinsically immune to stray capacitances [3, 4]. However, due to safety reasons and/or operating limitations of floating capacitive sensors, grounding one of the electrodes might be unavoidable in some applications, for example: the level measurement of a conductive liquid in a grounded metallic container [2, 5, 6] or the distance/proximity measurement to a grounded metallic object [7].

In recent years, interface circuits for floating capacitive sensors have undergone great progress, thus resulting in low-cost and accurate circuits that can easily be implemented in CMOS IC technology [8–12]. Such circuits apply many advanced measurement techniques (e.g. two-port measurement, auto-calibration and chopping) in order to reduce the uncertainty of the output information.

Interface circuits for grounded capacitive sensors have not undergone the same progress as those for floating capacitive sensors and few alternatives are available. The usual interface circuit is a simple RC oscillator implemented with either a 555 timer IC or an analogue comparator [2, 7, 13, 14]. When the sensor is remote from its electronics, such an RC oscillator applies the active-shielding technique (generally, by means of feedback control) to the interconnecting shielded cable [3]. However, this design solution shows a stability–accuracy trade-off [14]. Another interesting interface circuit for grounded capacitive sensors that applies active shielding based on feedforward techniques has been described in [15], although its performance is not reported and no advanced measurement techniques are applied. A modified bridge
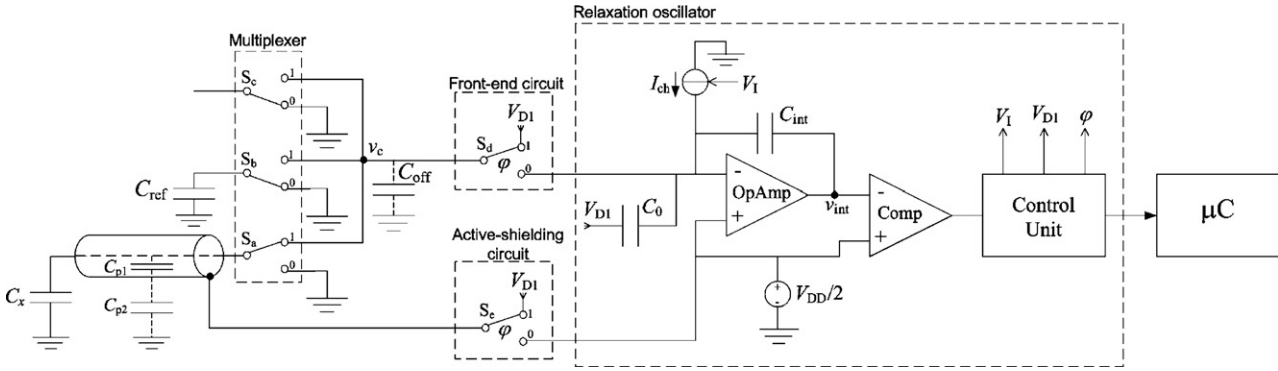
Figure 1. Schematic diagram of the novel interface circuit for grounded capacitive sensors.

circuit for grounded capacitive sensors intended for liquid-level measurements has been proposed in [6], but problems related to active shielding are not addressed.

This paper proposes a novel interface circuit for grounded capacitive sensors. The novel design adapts known measurement techniques (applied so far to floating capacitive sensors) to grounded capacitive sensors. Furthermore, such techniques are combined with feedforward-based active shielding.

2. Interface circuit

2.1. Overview of the circuit

Figure 1 shows a simplified schematic diagram of the novel interface circuit. The grounded capacitive sensor (C_x) is connected to the interface circuit through a shielded cable, which is driven by an active-shielding circuit (explained in section 2.3). A multiplexer (formed by three analogue switches S_a, S_b and S_c) selects the grounded capacitance to be measured, which can be: the sensor capacitance (C_x), a reference capacitor (C_{ref}) or the offset (stray) capacitance to ground (C_{off}). The selected capacitance is then connected to a charge-balanced relaxation oscillator through a front-end circuit (explained in section 2.2). Such an oscillator, which has been used before for floating capacitive sensors [10, 11], is formed by an operational amplifier (OpAmp) configured as an integrator, a comparator, a controlled current source (I_{ch}) and a control unit; the latter generates the digital control signals V_I, V_{D1} and φ. The oscillator provides a signal whose period (T_x, T_{ref} and T_{off}) is proportional to the grounded capacitance selected ($C_x + C_{off}$, $C_{ref} + C_{off}$ and C_{off}, respectively). Such periods are then directly measured by a microcontroller. Next, in order to compensate for offset and gain errors, the three-signal auto-calibration technique is applied by calculating the following ratio [10]:

$$M = \frac{T_x - T_{off}}{T_{ref} - T_{off}}. \tag{1}$$

From (1), the value of the sensor capacitance can be estimated by $C_x = M C_{ref}$.

2.2. Front-end circuit

Grounded capacitive sensors have one of the two electrodes grounded and, therefore, just one electrode is available for the measurement. Consequently, a one-port measurement must be performed instead of the usual two-port measurement applied to floating capacitive sensors [10, 11]. In order to do that, we propose the front-end circuit shown in figure 1. The circuit is just a switch (S_d) of 2-to-1 and works as follows. Initially, the grounded capacitance selected by the multiplexer (from now on, C) is connected to V_{D1}. If $V_{D1} =$ '1' then C is charged to the positive supply voltage (V_{DD}), however, if $V_{D1} =$ '0', then C is discharged to ground. Afterwards, C is connected to the integrator and, due to the virtual short circuit at the input of the OpAmp, a charge $Q = C V_{DD}/2$ is transferred from C to the feedback capacitance C_{int} (or from C_{int} to C, depending on the value of V_{D1}). This causes a negative (or positive) voltage step at the integrator output (v_{int}) equal to

$$\Delta v_{int} = \mp \frac{C V_{DD}}{2 C_{int}}. \tag{2}$$

Unlike the charge-transfer circuits for grounded capacitive sensors proposed in [3, 15], the front-end circuit in figure 1 can convert the sensor information to positive and negative signals (equation (2)). This enables the circuit to apply chopping techniques [10, 11], whose benefits are explained in section 2.3.

Figure 2 shows the control signals (φ and V_{D1}) of the front-end circuit together with the waveform of other relevant signals when a '$+ -, + -$' chopping sequence is applied. It shows how the voltage steps at v_{int} generated by C (equation (2)) are converted to time intervals $T_{s,i} (= C V_{DD}/(2|I_{ch}|))$ by integrating I_{ch} [10]. Figure 2 also shows the role of the capacitance C_0 (figure 1): it generates other voltage steps at v_{int} ($\Delta v_{int} = \mp C_0 V_{DD}/C_{int}$) that are converted to time intervals $T_{0,i} (= C_0 V_{DD}/|I_{ch}|)$ while C is sampling V_{D1} (i.e. when $\varphi = 1$). Consequently, the period T of the oscillator output signal in figure 2 equals

$$T = \frac{V_{DD}}{|I_{ch}|} (2C_0 + C), \tag{3}$$

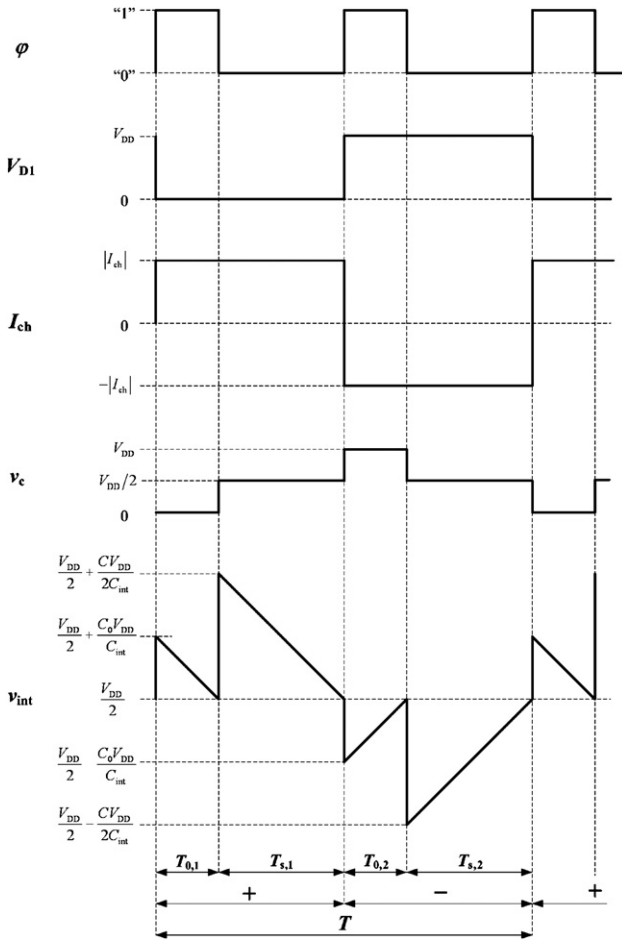which is proportional to the capacitance C selected by the multiplexer.

Figure 2. Waveform of some relevant signals of the circuit in figure 1 when a '+ −, + −' chopping sequence is applied.

2.3. Active-shielding circuit

The measurement of remote grounded capacitive sensors should be insensitive to the parasitic capacitances (C_{p1} and C_{p2} in figure 1) of the interconnecting shielded cable. To achieve such a goal, it is advisable to apply the active-shielding technique, which relies on having the potential of the cable shield equal to that of the inner conductor. The usual way to do so is by means of a feedback-based active shielding, which can easily be implemented with an OpAmp configured as a voltage follower [3]. Regrettably, such a solution shows a positive feedback path through the parasitic components that can bring about electronic instability [14].

An alternative way to have both potentials equal is by means of feedforward techniques. The basic idea is the following: if the values of potential applied to the inner conductor are known in advance, these can also be applied to the shield without the need of feedback. According to figure 2, the voltage v_c (which is that applied to the inner conductor) can be ground, $V_{DD}/2$ or V_{DD}. Therefore, a feedforward-based active shielding can easily be implemented with one switch S_e that is in phase with S_d [15], as shown in figure 1. This configuration ensures a shield potential equal to the inner potential and is stable since there is no feedback. This

technique is also insensitive to time delays in the operation of switches S_d and S_e. For example, if S_d changes to position 0 but S_e is still at position 1, then C_{p1} contributes a charge to C_{int}. However, such a charge flows back from C_{int} to C_{p1} when S_e changes to position 0 and, therefore, just C_x contributes in the effective charge transfer to C_{int}. In other words: it is not necessary that the shield potential follows the inner potential at any moment, but they must be the same at the end of each operating phase. Consequently, differences in the time constants of the RC circuits seen from switches S_d and S_e are not a problem either, whenever such time constants are much smaller than the interval time $T_{s,i}$ (figure 2).

Low-frequency non-idealities of the OpAmp in figure 1 (such as the input offset voltage and $1/f$ noise) can bring about a voltage difference across C_{p1} when C_x is connected to the integrator (i.e. when S_d and S_e are at position 0). This voltage difference across C_{p1} can affect the charge transfer to C_{int}. However, these effects are compensated in the time domain by means of the applied chopping technique (figure 2). Note that such effects cannot be compensated by the three-signal technique since only the sensor measurement suffers from them.

3. Materials and method

A prototype of the interface circuit shown in figure 1 has been built using a printed circuit board (PCB) with discrete components. The board was powered with a single supply voltage $V_{DD} = 5$ V. The multiplexer was implemented by a MAX4560, which includes three switches of 2-to-1. The switches of the front-end and active-shielding circuits were implemented by another MAX4560. The relaxation oscillator was realized by an OpAmp (OPA2350), a comparator (MAX987) and a controlled current source $I_{ch} = \pm 25$ μA. With such a current and the applied capacitors, the oscillator generated an output signal whose frequency was in the range of tens of kHz. The control unit, which was implemented by some simple digital gates, applied a '+ −, + −' chopping sequence, as shown in figure 2. The microcontroller was a PIC16F876 (Microchip) running on a clock frequency of 20 MHz, thus achieving a digital timing resolution of $T_s = 200$ ns. In order to reduce quantization effects, the microcontroller measured 128 consecutive periods of the oscillator output signal. The voltage $V_{DD}/2$ was obtained using a voltage divider and an OpAmp (AD8607) configured as a voltage follower; such an OpAmp is able to drive high-value capacitive loads.

The circuit in figure 1 was tested for sensor capacitances (C_x) between 27 pF and 330 pF (which is a typical range for capacitive liquid-level sensors [16]) and for different lengths of the interconnecting cable (up to 22 m). The sensor capacitance (C_x) was emulated by capacitors, whose actual values were measured by an impedance analyser (Agilent 4294A). The interconnecting cable was emulated by means of the capacitors C_{p1} and C_{p2} following the rule of thumb $c_{p1} = c_{p2} = 100$ pF m^{-1}, which is usual in triaxial cables in which the second shield is connected to ground. The rest of the capacitors of the circuit were $C_{ref} = 330$ pF, $C_{int} = 470$ pF and $C_0 = 47$ pF. All capacitors were NP0 ceramic.
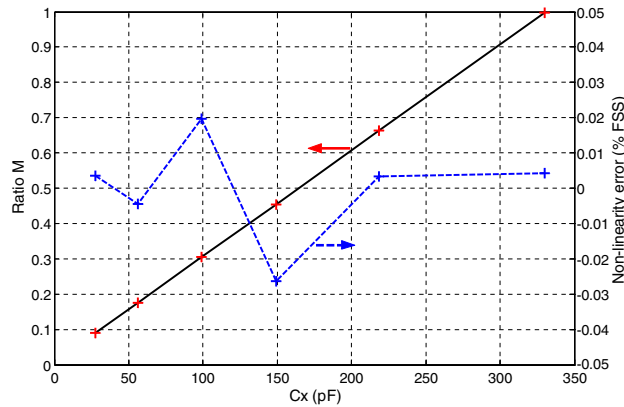
Figure 3. Experimental results of the linearity test for a 0 m interconnecting cable.
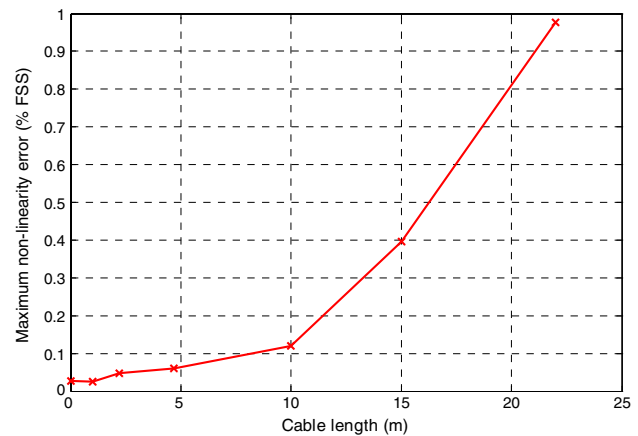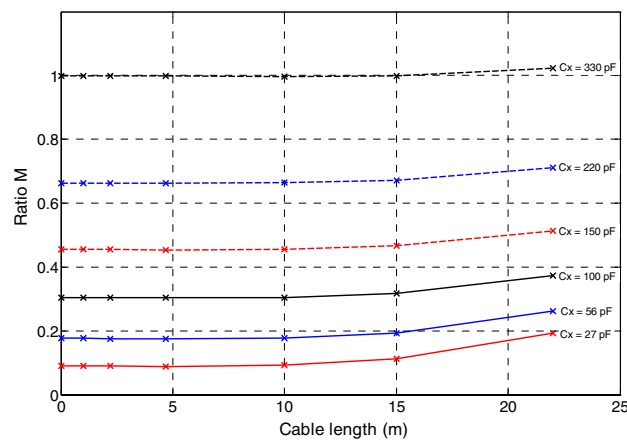

Figure 4. Ratio M versus the cable length for different values of C_x.

4. Experimental results and discussion

Figure 3 shows the ratio M, which is calculated as the mean of 100 values, for different values of C_x and for a 0 m interconnecting cable. It also shows the straight line fitted to the experimental data by means of the least-square method and the resultant nonlinearity error, which is expressed as a part of the full scale span (FSS). The measurement results show very good linearity, to be precise: the maximum nonlinearity error is about 0.026% FSS, which corresponds to 86 fF.

When the capacitors C_{p1} and C_{p2} were placed to emulate the interconnecting cable, the interface circuit did not become unstable. The period T_x (but not T_{ref} and T_{off}) and, hence, the ratio M were sensitive to C_{p1} and C_{p2}. Figure 4 shows how M depended on the cable length (ℓ) for different values of C_x. For $\ell \leqslant 10$ m, M is almost independent of ℓ, as expected. Nevertheless, for $\ell > 10$ m, M increases with ℓ, and such an increase is higher for low values of C_x. According to section 2.3, the reason for these errors under these conditions could be that the time constant seen from switch S_e (which is determined by a high-value C_{p2}) is comparable to the interval time $T_{s,i}$ (which is determined by a low-value C_x). Such effects can be reduced by (a) increasing $T_{s,i}$, which can be performed using a smaller I_{ch}, and/or (b) decreasing the time constant

Figure 5. Maximum nonlinearity error for various cable lengths.

seen from switch S_e, which can be carried out by selecting a switch with a smaller on-resistance.

According to the experimental results shown in figure 4, for high-accuracy applications it is advisable to perform the field calibration of the measurement system using the same cable length used in normal operating conditions. For this reason, we proceed to analyse the linearity of M versus C_x for each value of cable length tested. The experimental results are summarized in figure 5. The maximum nonlinearity error increases with the cable length, but it remains acceptable (i.e. less than 1% FSS). For example, the error equals 0.03% FSS, 0.06% FSS and 0.12% FSS for a 1 m, 5 m and 10 m interconnecting cable, respectively. These errors are much smaller than those obtained with the simple RC oscillator circuit with feedback-based active shielding [14]; for a 5 m and 10 m cable, the error is more than 30 times smaller. Therefore, the novel interface circuit is more stable and linear, although it is more complex as well.

For a measuring time of about 30 ms, the standard deviation of the ratio M was less than 50×10^{-6} and almost independent of both the sensor capacitance and the cable length. Over the full scale (i.e. $M = 1$), such a value of standard deviation corresponds to 14.3 bits of resolution. The referred measuring time includes all three measurements needed to perform the three-signal technique and is fully acceptable, for instance, for liquid-level measurements.

5. Conclusions

This paper has presented a novel interface circuit for grounded capacitive sensors. Two simple but effective switches (S_d and S_e in figure 1) determine most of the operation of the novel circuit. The first switch (S_d) enables the circuit to apply advanced measurement techniques (such as oscillator principles, auto-calibration and chopping) applied so far to floating capacitive sensors. The second switch (S_e) drives the interconnecting cable by applying feedforward-based active shielding, thus avoiding instability problems. In comparison to the simple RC oscillator circuit with feedback-based active shielding, the novel interface circuit is much more stable

and linear, although it is more complex as well. The ideas presented herein can be used to extend the capability of universal sensor interfaces towards the measurement of grounded capacitive sensors. Industrial applications, such as the water-level measurement at the bottom of oil tanks, can benefit from the results of this work.

Acknowledgments

References

[1] Puers R 1993 Capacitive sensors: when and how to use them *Sensors Actuators* A **37–38** 93–105
[2] Baxter L K 1997 *Capacitive Sensors. Design and Applications* (Piscataway, NJ: IEEE)
[3] Huang S M, Stott A L, Green R G and Beck M S 1988 Electronic transducers for industrial measurement of low value capacitances *J. Phys. E: Sci. Instrum.* **21** 242–50
[4] Marioli D, Sardini E and Taroni A 1993 High-accuracy measurement techniques for capacitance transducers *Meas. Sci. Technol.* **4** 337–43
[5] Ross P J 1983 A water-level sensor using a capacitance to frequency converter *J. Phys. E: Sci. Instrum.* **16** 827–8
[6] Bera S C, Ray J K and Chattopadhyay S 2006 A low-cost noncontact capacitance-type level transducer for a conducting liquid *IEEE Trans. Instrum. Meas.* **55** 778–86
[7] Haase W C 2004 Digital measurement circuit and system using a grounded capacitive sensor *US Patent* 6,700,392
[8] Kondo K and Watanabe K 1989 A switched-capacitor interface for capacitive sensors with wide dynamic range *IEEE Trans. Instrum. Meas.* **38** 736–9
[9] Kolle C and Leary P O 1998 Low-cost, high-precision measurement system for capacitive sensors *Meas. Sci. Technol.* **9** 510–7
[10] Goes F M L and Meijer G C M 1996 A novel low-cost capacitive-sensor interface *IEEE Trans. Instrum. Meas.* **45** 536–40
[11] Li X and Meijer G C M 2002 An accurate interface for capacitive sensors *IEEE Trans. Instrum. Meas.* **51** 935–9
[12] Bracke W, Merken P, Puers R and Van Hoof C 2005 On the optimization of ultra low power front-end interfaces for capacitive sensors *Sensors Actuators* A **117** 273–85
[13] Pallàs-Areny R and Webster J G 2001 *Sensors and Signal Conditioning* 2nd edn (New York: Wiley)
[14] Reverter F, Li X and Meijer G C M 2006 Stability and accuracy of active shielding for grounded capacitive sensors *Meas. Sci. Technol.* **17** 2884–90
[15] Herzog M 1988 Circuit for measuring capacitance by charging and discharging capacitor under test and its shield *US Patent* 4,743,837
[16] Reverter F, Li X and Meijer G C M 2007 Liquid-level measurement system based on a remote grounded capacitive sensor *Sensors Actuators* A **138** 1–8